

Supplementary material

**Palladium nanoparticles modified carbon spheres  
@ molybdenum disulfide core-shell composite for  
electrochemical detecting quercetin**

**Fubin Pei <sup>1</sup>, Yi Wu <sup>1</sup>, Shasha Feng <sup>1</sup>, Hualai Wang <sup>1</sup>, Guangyu He <sup>2</sup>, Qingli Hao <sup>1</sup> and Wu Lei <sup>1\*</sup>**

<sup>1</sup> School of Chemistry and Chemical Engineering, Nanjing University of Science and Technology, Nanjing 210094, JiangSu, China; peifubin@163.com (F.P.); wudayi@njust.edu.cn (Y.W.); fengshasha0319@163.com (S.F.); wanghualai@163.com (H.W.); qinglihao@njust.edu.cn (Q.H.); leiwuhao@njust.edu.cn (W.L.)

<sup>2</sup> Jiangsu Key Laboratory of Advanced Catalytic Materials and Technology, Changzhou University, 213164, China; hegy@cczu.edu.cn (G.H.)

\*: Corresponding author:

Tel.: +86-25-84315943; Fax: +86-25-84315190

Email address: leiwuhao@njust.edu.cn (W. Lei)

### *Reagents and apparatus*

Glucose, sodium molybdate dehydrate ( $\text{Na}_2\text{MoO}_4 \cdot 2\text{H}_2\text{O}$ ), ascorbic acid and citric acid were obtained from Aladdin Reagent Co., Ltd. (Shanghai, China). Thiourea, palladium chloride ( $\text{PdCl}_2$ ), potassium ferricyanide ( $\text{K}_4[\text{Fe}(\text{CN})_6]$ ), potassium ferrocyanide ( $\text{K}_3[\text{Fe}(\text{CN})_6]$ ), sodium dihydrogen phosphate ( $\text{NaH}_2\text{PO}_4$ ) and disodium hydrogen phosphate ( $\text{Na}_2\text{HPO}_4$ ) were purchased from Sinopharm Chemical Reagent Co., Ltd. (Beijing, China). Quercetin dehydrate, sodium borohydride ( $\text{NaBH}_4$ ), dextrin, sodium chloride and potassium chloride were purchased from Energy Chemical Co., Ltd. (Shanghai, China). Green tea and apple juice were obtained from local supermarket (Nanjing, China). Apple juice is 100% fresh apple juice without addition of preservative and sugar as indicated by the producers. Phosphate buffered saline (PBS, 1/15 M) was prepared by compounding the solution of  $\text{Na}_2\text{HPO}_4$  and  $\text{NaH}_2\text{PO}_4$ . The level of other chemicals and solvents were of analytical grade and were used without further purification. Ultrapure water ( $18.2 \text{ M}\Omega \text{ cm}$ ,  $24^\circ\text{C}$ ) was used in all the experimental processes. All the reagents were not further purified.

Scanning electron microscope (SEM) images were obtained at a FEI Quanta 250 FEG scanning electron microscope. Transmission electron microscope (TEM) images were obtained from a Tecnai G<sup>2</sup> F20 transmission electron microscope (FEI, America). Energy Dispersive X-Ray spectra (EDX) was recorded by JEOL JSM-6700F microscope (Japan). X-Ray photoelectron spectroscopy (XPS) data were measured using a Thermo ESCALAB 250 spectrometer with Al K $\alpha$  radiation (1486 eV). All the electrochemical measurement was carried on a CHI660D working station (Chenhua, Shanghai).

### *Preparation of Cs*

In particular, 4.0 g glucose was dissolved in 50 mL distilled water. After stirring for 10 min, the solution was placed in Teflon-sealed autoclave and heated up to  $180^\circ\text{C}$  for 4 h. Then cooled to room temperature, the product was isolated by centrifugation, washed with distilled water and ethanol, and dried at  $60^\circ\text{C}$  for 8 h.

### *Preparation of Cs@MoS<sub>2</sub>*

Simply, 20 mg Cs, 0.3 g  $\text{Na}_2\text{MoO}_4 \cdot 2\text{H}_2\text{O}$  and 0.6 g thiourea were introduced into 60 mL distilled water. After centrifugation for 20 min, the mixed solution was transferred into Teflon-sealed autoclave, kept at  $180^\circ\text{C}$  for 10 h. Then cooled to room temperature naturally,

the product was washed with distilled water and ethanol and dried at 60 °C for 8 h. The preparation of MoS<sub>2</sub> also used above step, only without Cs.

#### *Preparation of Cs@MoS<sub>2</sub>-Pd NPs*

Typically, 15 mg Cs@MoS<sub>2</sub> and 400  $\mu$ L PdCl<sub>2</sub> solution (20 mM) were introduced into 20 mL distilled water. After centrifugation for 20 min, the fresh 1.0 mL NaBH<sub>4</sub> solution (1 mM) was dropped into mixed solution. Then stirring 1 h, the product was isolated by centrifugation, washed with water and dried at 30 °C for 12 h.

#### *Characterization of Cs@MoS<sub>2</sub>-Pd NPs by FTIR, XRD, Raman, and Zeta potential*

FTIR spectra of the composites show in Figure S1A. All spectrum are included the peaks of 1700, 1590, and 1012 cm<sup>-1</sup> corresponding to C=O, C-C, and C-O bond. [1] The C=O bond of Cs@MoS<sub>2</sub> and Cs@MoS<sub>2</sub>-Pd NPs are weaker than that of Cs, due to its depletion by further hydrothermal reactions. Importantly, the peaks corresponding to S-S bond is observed at 904 cm<sup>-1</sup>, indicating that MoS<sub>2</sub> is successfully synthesized on Cs. [2] The Cs@MoS<sub>2</sub>-Pd NPs was confirmed by X-ray diffraction (XRD), as shown in Figure S1B. The broad peak of amorphous carbon is widely distributed especially around 20°. [3] Two weak peaks at 14.5° and 33.5° were attributed to the (002) and (100) crystal planes by indexing to crystalline MoS<sub>2</sub> (JCPDS card no. 37-1492). [4] And the weak peak at 38.5° was attributed to the (111) crystal planes by indexing to Pd. [5] The weak peaks may be caused by the inconspicuous crystal structure and low content. The peaks at 1350 and 1590 cm<sup>-1</sup> are considered to be typical D and G vibrational bands which are from the defect and disorder structures in carbon, and the graphitic in-plane vibrations of ideal sp<sup>2</sup> carbons, respectively. The peaks at 380 and 410 cm<sup>-1</sup> are corresponding to the E<sub>2g</sub><sup>1</sup> and A<sub>1g</sub> mode of the hexagonal MoS<sub>2</sub> crystal. [6] The Figure S1D shows that the apparent Zeta potentials of Cs, Cs@MoS<sub>2</sub> and Cs@MoS<sub>2</sub>-Pd NPs are negative, and more and more negative. The results show that the Cs@MoS<sub>2</sub>-Pd NPs are successfully prepared.

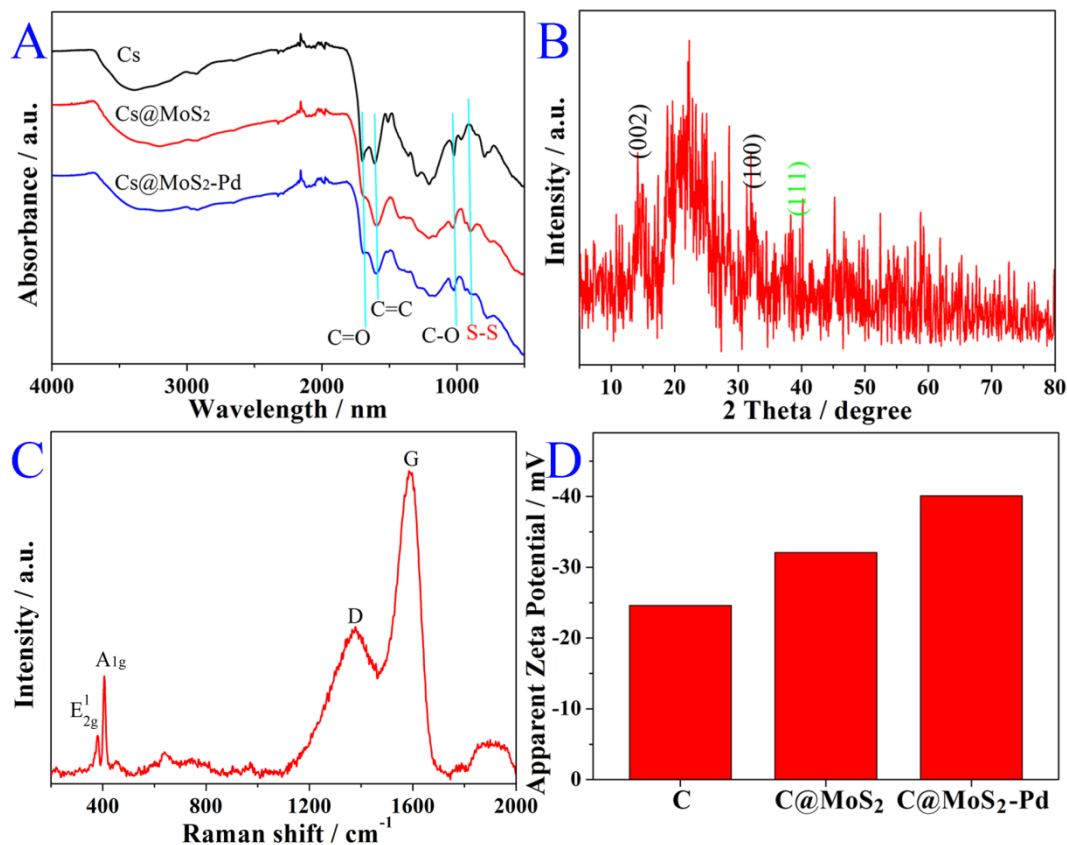


Figure S1. The IR (A) and apparent Zeta potential (D) of Cs, Cs@MoS<sub>2</sub> and Cs@MoS<sub>2</sub>-Pd NPs; XRD (B) and Raman spectroscopy (C) of Cs@MoS<sub>2</sub>-Pd NPs.

#### *The optimization of test conditions*

From the Figure 6A, it can be seen that the peak current response is largest, when the pH is 6.0. And its detailed current changes are shown in Figure S2A. It can be seen that the current response is biggest, when pH is 6.0. The strong acid will make MoS<sub>2</sub> inactive, thus strong acid condition Cs@MoS<sub>2</sub>-Pd NPs has low catalytic activity. While, alkaline conditions promote the hydrolysis of QR resulting low current response. Thus, the pH=6.0 was selected as the optimum condition.

The amount of Cs@MoS<sub>2</sub>-Pd NPs also influences the current signal, which is studied in Figure S2B. The current signal increases with the increase of the amount of Cs@MoS<sub>2</sub>-Pd NPs, which can be attributed to increasing active sites. Beyond 5.0  $\mu$ L, the current decreases, which may be is the  $R_{ct}$  increasing with the increase of Cs@MoS<sub>2</sub>-Pd NPs. Therefore, the Cs@MoS<sub>2</sub>-Pd NPs is most suitable for testing when the volume is 5.0  $\mu$ L.

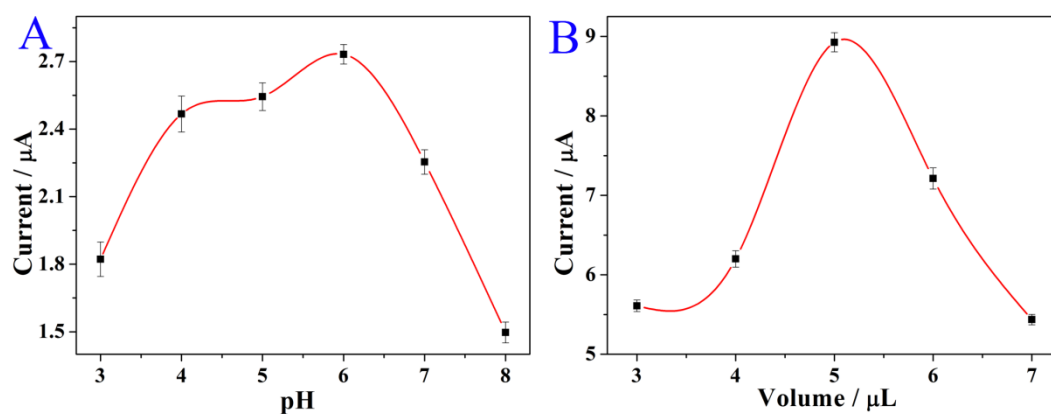


Figure S2 The he optimization of experimental conditions: pH of PBS (A) and amount of Cs@MoS<sub>2</sub>-Pd NPs (B)

**Table S1.** The analog datum of EIS.

Electrod e	R <sub>et</sub> (Ω)	R <sub>s</sub> (Ω)	CPE1-T	CPE1-P	W1-R	W1-T	W1-P
a	241	118.7	4.145E-6	0.871	579.6	0.296	0.487
b	1376	209.6	1.298E-5	0.705	831.4	0.506	0.346
c	1063	103.4	4.0E-5	0.619	391.3	0.373	0.937
d	418	184.2	5.999E-6	0.863	288.2	0.057	0.464

**Table S2.** The fitted equation and effective area (A).

Curve	Fitted equation	A
a	$Q = 0.2512 + 0.02t^{1/2}$ (r = 0.999)	$A_0$
b	$Q = 2.8253 + 0.12t^{1/2}$ (r = 0.999)	$1.504 A_0$
c	$Q = 7.887 + 39.99t^{1/2}$ (r = 0.999)	$1.997 A_0$
d	$Q = 7.353 + 51.53t^{1/2}$ (r = 0.999)	$2.574 A_0$

**Table S3.** Comparison with previous literature.

Signal amplification system	Method	Linear range ( $\mu\text{M}$ )	LOD (nM)	Reference
Glassy carbon electrode modified with the 3D SWCNTs-coumarin hybrid material	DPSV	0.25~3.0	20	[7]
1-Ethylpyridinium Bromide/Carbon Paste Composite Electrodepoly(vinylpyrrolidone)	DPV	0.25~7.43	44.8	[8]
Carbon-paste electrode modified with the polymer poly(vinylpyrrolidone)	SWV	0.5~5.5	170	[9]
ZnS quantum dots modified by mercaptoacetic acid	Fluorescence	2.65~7.50	571	[10]
Glassy carbon electrodes modified with MWCNT dispersed in poly(acrylic acid)	SWV	2.0~11	200	[11]
Cs@MoS <sub>2</sub> -Pd NPs	SWV	0.5~12	20	This work

**Table S4.** Detection of the HBs Ag in human serum samples with the proposed sensor

Samples	The addition content ( $\mu\text{g/mL}$ )	The detection content ( $\mu\text{g/mL}$ )	RSD (%, n=5)	Recovery (%)
Apple juice	0	1.33	2.97	---
	1.0	2.42	3.29	109
	3.0	4.49	4.27	105.3
	5.0	6.26	3.74	98.6
	0	1.74	3.27	---
Green tea	1.0	2.85	2.85	111
	3.0	4.57	3.29	94.3
	5.0	6.93	3.88	103.8

## Reference

1. Cheng, G. G.; Dong, L. J.; Kamboj, L.; Khosla, T.; Wang, X. D.; Zhang, Z. Q.; Guo, L. Q.; Pesika, N.; Ding, J. N., Hydrothermal Synthesis of Monodisperse Hard Carbon Spheres and Their Water-Based Lubrication. *Tribology Letters* **2017**, 65 (4).
2. Song, Y. J.; Cao, K. H.; Li, W. J.; Ma, C. Y.; Qiao, X. W.; Li, H. L.; Hong, C. L., Optimal film thickness of rGO/MoS<sub>2</sub> @ polyaniline nanosheets of 3D arrays for carcinoembryonic antigen high sensitivity detection. *Microchem J.* **2020**, 155.
3. Seo, J. C.; Umirov, N.; Park, S. B.; Lee, K.; Kim, S. S., Microalgae-derived hollow carbon-MoS<sub>2</sub> composite as anode for lithium-ion batteries. *Journal Of Industrial And Engineering Chemistry* **2019**, 79, 106-114.
4. Yu, X.; Shi, J. J.; Wang, L.; Wang, W. T.; Bian, J. J.; Feng, L. J.; Li, C. H., A novel Au NPs-loaded MoS<sub>2</sub>/RGO composite for efficient hydrogen evolution under visible light. *Materials Letters* **2016**, 182, 125-128.
5. Hu, Q. Y.; Zhang, R. H.; Chen, D.; Guo, Y. F.; Zhan, W.; Luo, L. M.; Zhou, X. W., Facile aqueous phase synthesis of 3D-netlike Pd-Rh nanocatalysts for methanol oxidation. *International Journal Of Hydrogen Energy* **2019**, 44 (31), 16287-16296.
6. Zhang, S. C.; Hu, R. R.; Dai, P.; Yu, X. X.; Ding, Z. L.; Wu, M. Z.; Li, G.; Ma, Y. Q.; Tu, C. J., Synthesis of rambutan-like MoS<sub>2</sub>/mesoporous carbon spheres nanocomposites with excellent performance for supercapacitors. *Applied Surface Science* **2017**, 396, 994-999.
7. Şenocak A, Köksoy B, Demirbaş E, Basova T, Durmuş M. 3D SWCNTs-coumarin hybrid material for ultra-sensitive determination of quercetin antioxidant capacity. *Sensors and Actuators B: Chemical* **2018**, 267:165-173
8. Tchieno FMM, Tonle IK, Njanja E, Ngameni E. A sensitive and low-cost analytical method for the electrochemical determination of quercetin, based on 1-ethylpyridinium bromide/carbon paste composite electrode. *International Journal of Chemistry* **2015**, 7 (2):27
9. Piovesan JV, Spinelli A. Determination of quercetin in a pharmaceutical sample by square-wave voltammetry using a poly (vinylpyrrolidone)-modified carbon-paste electrode. *Journal of the Brazilian Chemical Society* **2014**, 25 (3):517-525
10. Wu D, Chen Z. ZnS quantum dots-based fluorescence spectroscopic technique for the detection of quercetin. *Luminescence* **2014**, 29 (4):307-313
11. Gutiérrez F, Ortega G, Cabrera JL, Rubianes MD, Rivas GA. Quantification of quercetin using glassy carbon electrodes modified with multiwalled carbon nanotubes dispersed in polyethylenimine and polyacrylic acid. *Electroanalysis* **2010**, 22 (22):2650-2657